Npn GaN/InGaN Heterojunction Bipolar Transistors Using a Palladium-Based Contact

Yi-Che Lee*, Tsung-Ting Kao, Jeomoh Kim, Mi-Hee Ji, Theeradetch Detchphrom, Russell D. Dupuis, and Shyh-Chiang Shen

School of Electrical and Computer Engineering
Georgia Institute of Technology
777 Atlantic Drive NW, Atlanta, GA 30332-0250
* POC Phone: 404-385-8327 E-mail: ylee302@mail.gatech.edu

Keywords: InGaN, GaN, heterojunction bipolar transistors, HBT, III-nitride

6

Abstract

We report improved device stability on *npn* GaN/InGaN heterojunction bipolar transistors (HBTs) grown on sapphire substrates using a Pd-based *p*-type contact scheme. When stressed at a constant base current, HBTs with Ni-based contact degraded quickly. High knee voltage and lowered current gain were observed, suggesting that the stressing leads to leaky base-collector junctions. On the other hand, stable device operation can be obtained in HBTs with Pd-based *p*-type contacts. The current gain of 80, a collector current density of >95 kA/cm^2 and a d.c. power handling capability of >1.3 MW/cm^2 were measured on post-stressed GaN/InGaN HBTs with Pd-based contact. To the best of our knowledge, the results are the highest d.c. device performance reported on III-N HBTs grown on sapphire substrates.

INTRODUCTION

III-nitride (III-N) materials system and related transistors offer greatly increased power-switching performance and dramatic theoretical advantages over other conventional semiconductor material systems. Although extensive efforts were spent on the development of III-N unipolar devices such as heterojunction field-effect transistors, recent developments of III-N heterojunction bipolar transistors (HBTs), in particular GaN/InGaN HBTs, have shown that III-N bipolar transistors could be suitable for next-generation high-power switching and amplification. *npn* III-N HBTs were successfully demonstrated with good current gain and high breakdown voltage **[**1-3**]**.High-temperature operation up to 300C has also been demonstrated [2].Previously, we have reported *npn* GaN/$In_{0.03}Ga_{0.97}N$ HBTs with high current gain ($h_{fe}= dI_C/dI_B$ > 84) and high current density ($J_C = I_C/A_E$ > 20 kA/cm^2) for devices grown on sapphire substrates [4]. Ultra-high d.c. power density ($P_{d.c.} = I_C \times V_{CE} / A_E$ >3 MW/cm^2) and high temperature operation was also reported for *npn* GaN/$In_{0.03}Ga_{0.97}N$ HBTs grown on free-standing GaN (FS-GaN) substrates [5,6]. The microwave performance of InGaN/GaN HBTs with f_T = 8 GHz were recently reported [7]. These devices however are subject to premature degradation and often results in reduced current gain under high current stressing conditions. Resistive base contact and leaky base-collector (BC) junction were observed after degradation. As a result, the achievable J_C and $P_{d.c.}$ were limited for GaN/InGaN HBTs, especially for the HBTs grown on sapphire substrates.

In this paper, we report an improvement in GaN/InGaN HBT performance stability using a Pd-based metallization for the base layer contacts. When compared to a typical Ni-based *p*-type contacts, the Pd-based *p*-type contact shows improved stability and is less susceptible to the high-current-stressing related device degradation. The fabricated GaN/InGaN HBTs showed a collector current density (J_C) > 95 kA/cm^2 and power density ($P_{d.c.}$) > 1.3 MW/cm^2 for a device with the emitter area (A_E) of 11.7 μm^2. To the best of our knowledge, the results represent the highest current density and power handling performance achievable for III-N HBTs grown on sapphire substrates to date.

LAYER STRUCTURE AND DEVICE FABRICATION

The layer structure of the *npn* GaN/$In_{0.03}Ga_{0.97}N$ HBTs were grown on a sapphire substrate in a Thomas–Swam metal–organic chemical vapor deposition (MOCVD) reactor. Detailed epitaxial growth techniques were similar to our earlier report [8]. The epitaxial layer grown on a sapphire substrate starts from a 2-μm-thick un-intentionally doped GaN buffer layer, followed by 880-nm Si-doped n-GaN sub-collector layer (free carrier concentration n = 4×10^{18} cm^{-3}), a 320-nm n-GaN collector layer (n = 1.0×10^{16} cm^{-3}), a 30-nm $In_xGa_{1-x}N$ (x = 0 – 0.03) collector-grading layer, a 110-nm Mg-doped $In_{0.03}Ga_{0.97}N$ base layer (p = 1 × 10^{18} cm^{-3}), a 30-nm $In_xGa_{1-x}N$ (x = 0.03 – 0) emitter-grading layer, and a 200-nm Si-doped n$^+$-GaN emitter cap layer (n = 1×10^{19} cm^{-3}).

The HBT fabrication starts with two steps of chlorine-based etching processes using an STS inductive-coupled plasma (ICP) etching system to form the emitter mesa and the base/collector mesa, respectively, for subsequent base and collector metal contacts. The wafer piece is treated with a diluted $KOH/K_2S_2O_8$ solution under the ultraviolet illumination to remove the etching-induced damage and to retain smooth surface [9]. Ti/Al/-based metal stacks were used for the emitter and the collector ohmic contact layers. Either Ni-based or the Pd-based *p*-type contact were deposited on two samples under study, respectively. After the metallization, the samples were passivated by a spin-on-glass. The via-holes were opened by ICP etching and a 1-µm-thick Ti/Au interconnect layer is deposited to complete the fabrication processing.

RESULTS AND ANALYSIS

The fabricated GaN/InGaN HBTs with Ni-based and Pd-based *p*-type contacts were measured by a Keithley SCS-4200 semiconductor analyzer at room temperature. In Figure 1, a current stressing test is shown by monitoring the change of the base-emitter voltage (V_{BE}) on two GaN/InGaN HBTs with the same emitter area (A_E = 20 × 20 µm^2) but different *p*-type base contact schemes (i.e., Ni-based and Pd-based p-contact metal.) A constant I_B of 100 µA and V_{CE} of 10 V were chosen for the stressing condition in these tests. The V_{BE} of the Ni-based HBT became unstable and a large amount of voltage drop was observed when the stress time is greater than 10 min. The reduced V_{BE} is attributed to the formation of additional leakage path during the base current stressing. Comparing the common-emitter family curves before and after stressing shown in Figure 2, the offset voltage (V_{offset}) and the knee voltage (V_{knee}) of the HBT were also increased by 2 V. The d.c current gain ($\beta = I_C/I_B$) was reduced slightly from 20 to 19 after the degradation occurred. Further study indicates that the device degradation is permanent and leads to a leaky BC junction at reverse bias. The leaky BC junction may be attributed to the enhanced electromigration of the metal species in the etched *p*-type base layer at high junction temperature during current stressing. Additional conduction paths were formed between the base metal contact and the underlying extrinsic collector region, which leads to increased offset voltage and device performance degradation. It further limited the achievable d.c. power handling capability of GaN/InGaN HBTs grown on sapphire substrates.

On the other hand, HBTs with Pd-based *p*-type contact show lower V_{BE} than that of Ni-based contacts in Figure 1. The lower V_{BE} indicates that Pd-based *p*-type contact layer can provide lower access resistance than the Ni-based contact, although they are not ohmic. The V_{BE} remains relatively stable (ΔV_{BE} < 17 mV) over a 1-hour constant current stressing, indicating no significant contact property changes during the current stressing. The stable base contact properties may be attributed to low diffusion coefficient of Pd in the *p*-type InGaN layer [10]. After the stressing, the measured common-emitter family curves shows similar V_{offset} and V_{knee} while the current gain is increased from 40 to 52 in Figure 3. The improved current gain can be attributed to the burn-in effect with a reduced hydrogen passivation in the InGaN base layer [11].

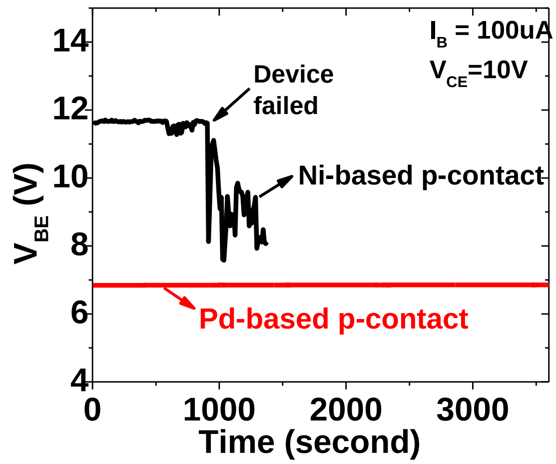

Figure 1 The time evolution of V_{BE} for GaN/InGaN HBTs under a constant I_B stressing condition in the forward active mode. The devices under test have A_E = 20 × 20 µm^2 and I_B = 100 µA at V_{CE} = 10 V.

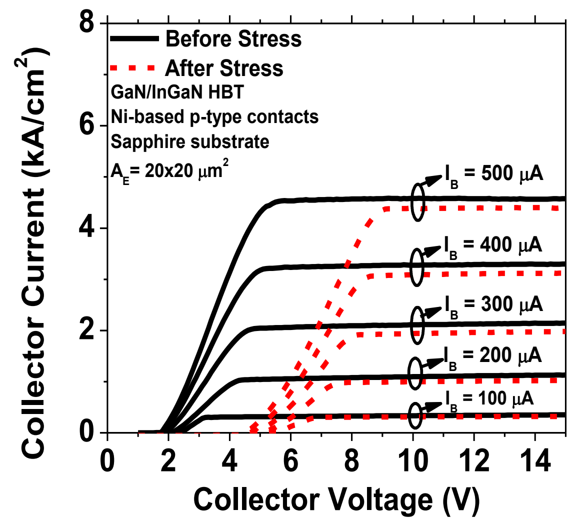

Figure 2 The common-emitter family curves of a GaN/InGaN *npn* HBT with Ni-based *p*-type base contacts before and after the constant-base-current stressing.

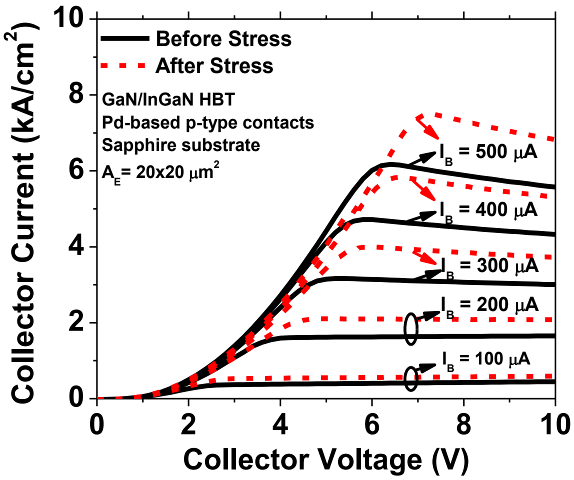

Figure 3 The common-emitter family curves of a GaN/InGaN HBT with Pd-based *p*-type contacts before and after the 1 hour constant-base-current stress

With the Pd-based *p*-type contacts, small-area (A_E = 11.7 μm^2) GaN/InGaN HBTs can handle much higher current than those with Ni-based contacts. A comparison of the Gummel plots of the devices using Ni and Pd-based *p*-type contact, respectively, are shown in Figure 4. I_B and I_C cross over at ~1 μA for HBT with Ni-based and Pd-based contacts, respectively. The cross-over voltage is at V_{BE} = 7 V for HBT with Ni-based contacts and 4V for HBT with Pd-based contacts. The lower cross-over point in V_{BE} is due to lower base resistance of Pd-based contacts. Beyond the cross-over point, the current gain (h_{fe} = dI_C/dI_B) reached maximum values of 80 at V_{BE} = 14V and 9 V, respectively. These results indicate that the base resistance is reduced by using the Pd-based contacts.

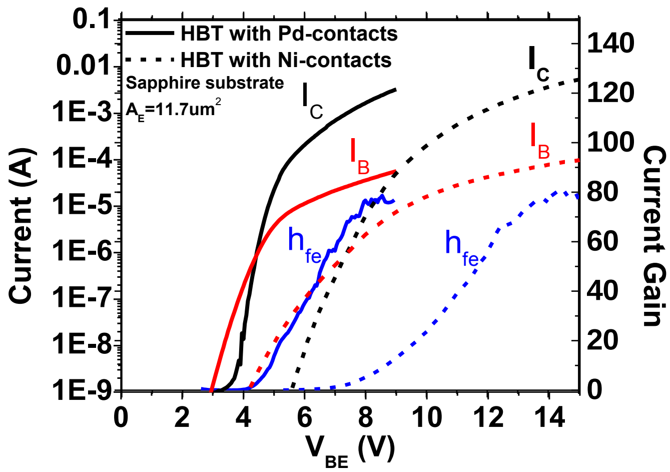

Figure 4 The Gummel plot of a GaN/InGaN HBT with A_E=11.7um^2 using Ni and Pd-based *p*-type contacts.

To explore the achievable J_C and $P_{d.c.}$ of GaN/InGaN HBTs with Pd-based contacts, a quasi-static measurement is conducted using an Agilent B1505 curve tracer. The pulsed base current has 1-ms pulse width and a repetition rate of 2 Hz (Duty cycle of 2%). The measured common-emitter characteristics are shown in Figure 5. With reduced joule heating and better stability of Pd in high current operation, J_C > 95 kA/cm^2 are achieved for HBT with Pd-based contacts at V_{CE} = 10 V without device degradation. The achievable $P_{d.c.}$ of > 1.3MW/cm^2 was also obtained at V_{CE} = 15 V. In contrast, HBTs with Ni-based contacts can only achieve J_C = 50 kA/cm^2 before the HBT failed. It is also noted that V_{offset} and V_{knee} of HBT with Pd-based contacts are lower than that of HBT with Ni-based contacts. The results suggest that GaN/InGaN HBTs with Pd-based *p*-type contacts are capable of achieving higher-power density handling capability even on substrates with poor thermal conductivity such sapphire.

6

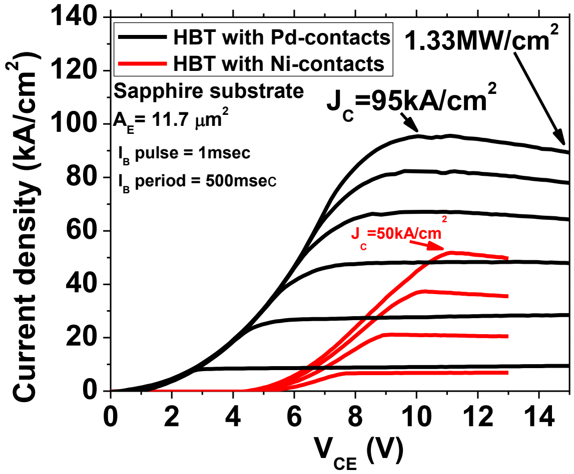

Figure 5 The quasi-static common-emitter family curves of GaN/InGaN HBT with Ni and Pd-based *p*-type base contacts

In Figure 6, a competitive chart summarizes the reported maximum current density (J_C) versus the current gain (h_{fe}) for GaN/InGaN HBTs grown on sapphire and SiC substrates. *Pnp* HBTs are also included in this chart for comparison. In this chart, both of the GaN/InGaN HBTs with Ni-based and Pd-based *p*-type contacts fabricated in Georgia Tech show state-of-the-art high current density with twice higher current gain than other GaN/InGaN HBTs. To our best knowledge, the results are the best device performance of III-N HBTs on sapphire substrates to date.

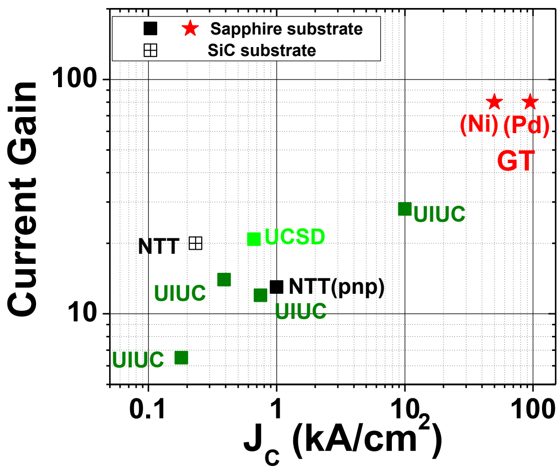

Figure 6 The maximum current density (J_C) and maximum current gain for GaN/InGaN HBTs [1,2,12-14].

CONCLUSIONS

In conclusion, we report a significant performance improvement in GaN/InGaN HBTs grown and fabricated on sapphire substrates using a Pd-based *p*-type contact. The Pd-based *p*-type contact shows better device stability when compared to Ni-based *p*-type contact. With the Pd-based contacts, the fabricated HBTs exhibit $h_{fe} > 80$, $J_C >$ 95 kA/cm^2 and $P_{d.c.} >$ 1.3 MW/cm^2. The improved metal contact stability enables a state-of-the-art high-power-density performance demonstration of GaN/InGaN HBTs, suggesting great potential of GaN/InGaN HBTs for next-generation high-power amplification and high-temperature applications.

ACKNOWLEDGEMENTS

The authors are thankful for the cleanroom facility support of the staff in the Nanotechnology Research Center (NRC) at the Georgia Institute of Technology in Atlanta, GA.

REFERENCES

[1] T. Makimoto, et al., Appl. Phys. Lett., 79, 380 (2001).
[2] D. Keogh, et al., Electron. Lett 42,661 (2006).
[3] J. J. Huang, et al., IEEE Electron Device Lett., **22**,157 (2001).
[4] Y. Zhang, et al., Phys. Status Solidi C **8**, 2451 (2011).
[5] S.-C. Shen, et al., IEEE Electron Dev. Let. **32**, 1065 (2011).
[6] Y.-C. Lee, et al., Phys. Status Solidi A **209**, 497 (2012).
[7] R. D. Dupuis, et al., ECS Transactions **58**, 261 (2013).
[8] Z. Lochner, et al., J. Crystal. Growth **315**, 278 (2011).
[9] Y. Zhang, et al., *A surface treatment technique for III-V device fabrication*, 2008 International Conference on Compound Semiconductor Manufacturing Technology Chicago, IL, pp. 13.3. (2008).
[10] H.K. Cho, et al., Solid-State Electron. **49**, 774 (2005).
[11] Y.-C. Lee, et al., IEEE Trans. Electron Dev. **57**, 2964 (2010).
[12] K. Kumakura, et al., phys. stat. sol. (a) **204**, 2037(2007)
[13] B. F. Chu-Kung, et al., Appl. Phys. Lett. **91**, 232114(2007)
[14] T. Chung, et al., Appl. Phys. Lett. **88**, 183501(2006)

ACRONYMS:

HBT : heterojunction bipolar transistor